Photonic crystal fiber sensor array based on modes overlapping

Guillermo A. Cárdenas-Sevilla,[1,2] Vittoria Finazzi,[2] Joel Villatoro,[2*] Valerio Pruneri[2,3]

[1] *Centro de Investigaciones en Óptica A. C. Loma del Bosque 115, León GTO. 37150 México*
[2]*ICFO-Institut de Ciencies Fotoniques, Mediterranean Technology Park, 08860 Castelldefels (Barcelona), Spain*
[3]*Also with ICREA-Institució Catalana de Recerca i Estudis Avançats, 08010, Barcelona, Spain*
**joel.villatoro@icfo.es*

Abstract: An alternative method to build point and sensor array based on photonic crystal fibers (PCFs) is presented. A short length (in the 9-12 mm range) of properly selected index-guiding PCF is fusion spliced between conventional single mode fibers. By selective excitation and overlapping of specific modes in the PCF we make the transmission spectra of the sensors to exhibit a single and narrow notch. The notch position changes with external perturbation which allows sensing diverse parameters. The well-defined single notch, the extinction ratio exceeding 30 dB and the low overall insertion loss allow placing the sensors in series. This makes the implementation of sensor networks possible.

OCIS codes: (060.5295) Photonic crystal fibers; (060.4005) Microstructured fibers; (060.2370) Fiber optics sensors; (280.4788) Optical sensing and sensors; (060.4230) Multiplexing.

References and links

1. J. M. Lopez-Higuera, ed., *Handbook of Optical Fiber Sensing Technology*, (Wiley, New York, 2002).
2. P. St. J. Russell, "Photonic-crystal fibers," J. Lightwave Technol. **24**(12), 4729–4749 (2006).
3. Y. Zhu, P. Shum, H. W. Bay, M. Yan, X. Yu, J. Hu, J. Hao, and C. Lu, "Strain-insensitive and high-temperature long-period gratings inscribed in photonic crystal fiber," Opt. Lett. **30**(4), 367–369 (2005).
4. C. Martelli, J. Canning, N. Groothoff, and K. Lyytikainen, "Strain and temperature characterization of photonic crystal fiber Bragg gratings," Opt. Lett. **30**(14), 1785–1787 (2005).
5. Y. Wang, H. Bartelt, W. Ecke, R. Willsch, J. Kobelke, M. Kautz, S. Brueckner, and M. Rothhardt, "Sensing properties of fiber Bragg gratings in small-core Ge-doped photonic crystal fibers," Opt. Commun. **282**(6), 1129–1134 (2009).
6. V. M. Churikov, V. I. Kopp, and A. Z. Genack, "Chiral diffraction gratings in twisted microstructured fibers," Opt. Lett. **35**(3), 342–344 (2010).
7. W. J. Bock, J. Chen, P. Mikulic, T. Eftimov, and M. Korwin-Pawlowski, "Pressure sensing using periodically tapered long-period gratings written in photonic crystal fibres," Meas. Sci. Technol. **18**(10), 3098–3102 (2007).
8. L. Rindorf and O. Bang, "Sensitivity of photonic crystal fiber grating sensors: biosensing, refractive index, strain, and temperature sensing," J. Opt. Soc. Am. B **25**(3), 310–324 (2008).
9. J. Villatoro, V. P. Minkovich, V. Pruneri, and G. Badenes, "Simple all-microstructured-optical-fiber interferometer built via fusion splicing," Opt. Express **15**(4), 1491–1496 (2007).
10. J. Villatoro, V. Finazzi, V. P. Minkovich, V. Pruneri, and G. Badenes, "Temperature-insensitive photonic crystal fiber interferometer for absolute strain sensing," Appl. Phys. Lett. **91**(9), 091109 (2007).
11. W. Bock, T. Eftimov, P. Mikulic, and J. Chen, "An inline core-cladding intermodal interferometer using a photonic crystal fiber," J. Lightwave Technol. **27**(17), 3933–3939 (2009).
12. Q. Shi, Z. Wang, L. Jin, Y. Li, H. Zhang, F. Lu, G. Kai, and X. Dong, "A hollow-core photonic crystal fiber cavity based multiplexed Fabry-Pérot interferometric strain sensor system," IEEE Photon. Technol. Lett. **20**(15), 1329–1331 (2008).
13. H. Y. Fu, A. C. L. Wong, P. A. Childs, H. Y. Tam, Y. B. Liao, C. Lu, and P. K. A. Wai, "Multiplexing of polarization-maintaining photonic crystal fiber based Sagnac interferometric sensors," Opt. Express **17**(21), 18501–18512 (2009).
14. D. Barrera, J. Villatoro, V. P. Finazzi, G. A. Cárdenas-Sevilla, V. P. Minkovich, S. Sales, and V. Pruneri, "Low-loss photonic crystal fiber interferometers for sensor networks," J. Lightwave Technol. **28**, 3542–3547 (2010).
15. K. Abe, Y. Lacroix, L. Bonnell, and Z. Jakubczyk, "Modal interference in a short fiber section: fiber length, splice loss, cutoff, and wavelength dependences," J. Lightwave Technol. **10**(4), 401–406 (1992).
16. A. Kumar and R. K. Varshney, "Transmission characteristics of SMS fiber optic sensor structures," Opt. Commun. **219**(1-6), 215–219 (2003).
17. Q. Wang, G. Farrell, and W. Yan, "Investigation on single-mode–multimode–single-mode fiber structure," J. Lightwave Technol. **26**(5), 512–519 (2008).
18. S. Silva, J. L. Santos, F. X. Malcata, J. Kobelke, K. Schuster, and O. Frazão, "Optical refractometer based on large-core air-clad photonic crystal fibers," Opt. Lett. **36**(6), 852–854 (2011).

#142479 - $15.00 USD Received 10 Feb 2011; revised 26 Mar 2011; accepted 28 Mar 2011; published 5 Apr 2011

19. Y. Jung, S. Kim, D. Lee, and K. Oh, "Compact three segmented multimode fibre modal interferometer for high sensitivity refractive-index measurement," Meas. Sci. Technol. **17**(5), 1129–1133 (2006).
20. W. S. Mohammed, P. W. E. Smith, and X. Gu, "All-fiber multimode interference bandpass filter," Opt. Lett. **31**(17), 2547–2549 (2006).
21. E. Li, "Temperature compensation of multimode-interference-based fiber devices," Opt. Lett. **32**(14), 2064–2066 (2007).
22. F. Pang, W. Liang, W. Xiang, N. Chen, X. Zeng, Z. Chen, and T. Wang, "Temperature-insensitivity bending sensor based on cladding-mode resonance of special optical fiber," IEEE Photon. Technol. Lett. **21**(2), 76–78 (2009).
23. J. E. Antonio-Lopez, A. Castillo-Guzman, D. A. May-Arrioja, R. Selvas-Aguilar, and P. Likamwa, "Tunable multimode-interference bandpass fiber filter," Opt. Lett. **35**(3), 324–326 (2010).
24. H. Liu, F. Pang, H. Guo, W. Cao, Y. Liu, N. Chen, Z. Chen, and T. Wang, "In-series double cladding fibers for simultaneous refractive index and temperature measurement," Opt. Express **18**(12), 13072–13082 (2010).
25. L. Xiao, M. S. Demokan, W. Jin, Y. Wang, and C. L. Zhao, "Fusion splicing photonic crystal fibers and conventional single-mode fibers: microhole collapse effect," J. Lightwave Technol. **25**(11), 3563–3574 (2007).
26. H. P. Uranus, "Theoretical study on the multimodeness of a commercial endlessly single-mode PCF," Opt. Commun. **283**(23), 4649–4654 (2010).

1. Introduction

Optical-fiber-based sensors represent a unique or the only viable sensing solution in specific cases (e.g., in environments with electrical hazard or potentially explosive). In addition, fiber sensors are a premium choice when multiplexing capability, high sensitivity and reduced size are required. For example, the multiplexing capability of fiber sensors makes it possible to monitor the individual behavior of several sensors set in a network with a single interrogation unit. This simplifies the design of a sensor network and minimizes its cost.

Sensors based on conventional optical fibers are well established [1], while those based on photonic crystal fibers (PCFs) are attracting considerable attention. PCFs are fibers with unique optical properties which are conferred by a periodic microstructure present all over the fiber length [2]. Their modal and guidance properties make PCFs appealing for optical sensing. So far a number of PCF sensors have been proposed, however, we believe that those based on Bragg gratings [3–6], long-period gratings [7,8] and interferometers [9–11] are the most promising ones for practical applications due their robustness. Most of these sensors have centimeter lengths and exhibit remarkable performance such as high stability over time, operation in a broad wavelength range or at extreme temperatures. However, they typically operate as point or single sensor [3–11]. The multiplexing of the PCF sensors based on gratings or interferometers proposed until now is not simple as demonstrated by some groups, including ours [12–14], largely because of the output signal of the sensors themselves, the lack of passive PCF devices and the high insertion loss that PCF sensors typically exhibit (10 dB or more). The multiplexing of PCF-based sensors is a necessary step to widen their capabilities. In this way, PCF sensors can compete with their well-established counterparts based on standard optical fibers.

In this work we propose a technique to build PCF point sensors which can be easily multiplexed to form sensor arrays or networks. The sensors are simple and consist of a stub of properly selected index-guiding PCF fusion spliced between conventional single mode fibers (SMF). Our devices fall into the category of single mode-multimode-single mode (SMS) devices, of which many variants have been proposed in the literature, see for example [15–24]. In our case, the voids of the PCF are sealed over an adequate length in the PCF-SMF interface. This induces a longitudinal offset allowing the efficient excitation and overlapping of specific modes in the PCF. As a consequence, the transmission spectrum of the devices exhibits a single and narrow notch at a resonant wavelength. Minute changes in the modal index or in the fiber length, caused for example by temperature or strain, result in a detectable shift of the notch position. When *n* sensors are set in cascade, the transmission of the series exhibits *n* dips. The dips are independent from each other, thus a shift in one of them does not

#142479 - $15.00 USD Received 10 Feb 2011; revised 26 Mar 2011; accepted 28 Mar 2011; published 5 Apr 2011

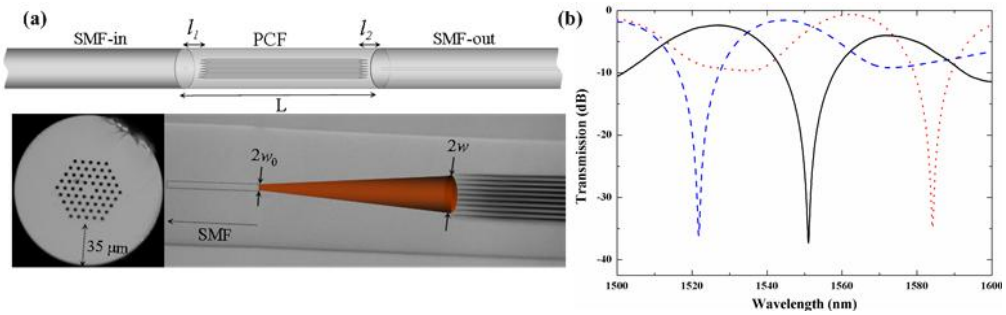

Fig. 1. (a) Scheme of the proposed device, micrograph of the PCF cross section and of a splice with a 200 µm-long collapsed zone. The broadening of the beam is illustrated by the red cone. L is the PCF length, l_1 and l_2 are the lengths of the collapsed regions. w_0 and w are the beam radius at the beginning and at the end of the collapsed region, respectively. (b) Transmission spectra of some devices with L = 10.42 mm (dashed line), 10.16 mm (solid line) and 11.02 mm (dotted line).

perturb the others. This allows the implementation of simple but functional PCF-based sensor arrays, and eventually of more complex sensor networks. The demodulation of the array is straightforward since the position of each notch can be monitored with commercially available equipment such as FBG interrogators or miniature spectrophotometers.

We believe that due to their simple multiplexing, sensitivity, compactness and low cost the PCF sensors proposed here can compete with other PCF sensors based gratings or interferometers and with SMF structures built with conventional fibers.

2. Device operating principle and sensing properties

The illustration of the device along with the cross section of the fiber used in the experiments is shown in Fig. 1. The fiber is a commercially available PCF which has six-fold symmetry; it is known as large-mode-area PCF (LMA-10, NKT Photonics). The fiber has a core size diameter of 10 µm, voids with diameter of 3.1 µm, pitch of 6.6 µm and outer diameter of 125 µm. To fabricate the devices, the PCF and the standard fiber (SMF-28) can be spliced with any commercial fusion splicing machine. In general, splicing machines join two fibers together making first a prefusion in which the fibers are cleared by low-level heating. After the prefusion a main fusion process follows in which the two fiber ends are exposed to an intense discharge (high temperature) for a few seconds. During the main fusion process the fiber are pushed and pulled to form a robust and permanent join. Because of the holey structure the softening point of PCFs is in general lower than that of SMFs. Thus, if an SMF and a PCF are spliced with a default program for splicing single mode fibers the PCF's air holes will entirely collapse over a certain length. In most splicing machines the intensity and duration of the arc discharge of the main fusion process can be adjusted. Thus, one can control the length of the collapsed zone in the PCF. We fabricated a collection of samples with a commercial fusion splicing machine (Ericsson FSU 955). To control the length of the collapsed zone we followed the technique reported in [25]. We found out that when the collapsed regions had different lengths, e.g., ~200 ± 10 µm in the PCF-SMF-in interface and ~110 ± 10 µm in the PCF-SMF-out one, the transmission spectrum of the device exhibits a single and deep notch, see Fig. 1. It can be seen from the figure that the notches are very narrow and that the insertion loss is small around the resonance wavelength. Note also that the position of the notch can be controlled with the length of PCF. Later we will see that these attributes simplify the multiplexing of the devices.

To elucidate the behavior of the devices let us consider the evolution of the propagating beam as it travels from the SMF-in, through the PCF, to the SMF-out. When the fundamental SMF-in mode enters the collapsed region of the PCF it immediately begins to diffract, and consequently, the mode broadens. If w_0 is the spot size at the SMF-in-PCF interface at a wavelength λ, see Fig. 1, then after propagating a length l_1 of collapsed region the spot size will be:

#142479 - $15.00 USD Received 10 Feb 2011; revised 26 Mar 2011; accepted 28 Mar 2011; published 5 Apr 2011

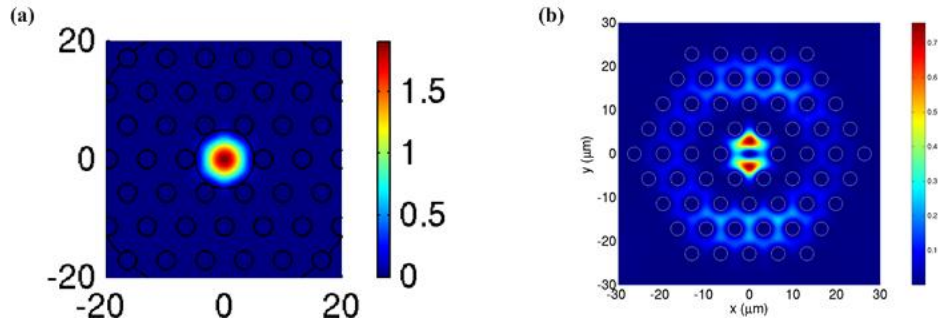

Fig. 2. (a) Calculated longitudinal component of the time-averaged Poynting vector of the fundamental HE_{11} mode (the x and y scales are in μm) and the HE_{22}-like cladding mode (b) at 1550 nm. The parameters of PCF (LMA-10) are described in the text.

$$w = w_0\sqrt{1+\left(\lambda l_1/\pi n_f w_0^2\right)^2}, \tag{1}$$

n_f being the refractive index of the collapsed region (solid silica fiber). Let us assume the following realistic values: λ = 1550 nm, l_1 = ~200 μm, n_f = 1.444 (silica), and w_0 = 5 μm. Under these conditions the PCF will be excited with a Gaussian beam whose size is $2w$ = ~30 μm i.e., with a light spot larger than the PCF core size. The mode field mismatch combined with the modal characteristics of the PCF (see, e.g., Ref [26].) allows the excitation of specific modes in the PCF. Owing to the axial symmetry and the longitudinal offset introduced by the collapsed region the excited modes are those that have similar azimuthally symmetry, i.e., the HE_{11} core mode and probably the HE_{22}-like cladding mode, also called quasi-HE_{22} cladding mode resonance [26]. To support this mechanism, in Fig. 2 we show the calculated longitudinal component of the time-averaged Poynting vector of the fundamental core mode and the HE_{22}-like cladding mode, both for a wavelength of λ = 1550nm. The simulations were carried out using commercial software (Comsol Multiphysics). From Fig. 2 it can be noted that the field of the HE_{22}-like mode penetrates the entire core mode area; therefore it strongly overlaps with the fundamental HE_{11} core mode.

The excited modes broaden when they enter the collapsed region in the PCF-SMF-out section because of diffraction. The type of modes excited in the PCF combined with an adequate broadening of the modes, i.e., an adequate length of collapsed region in the PCF, is what produces a single dip in the device transmission. It was experimentally observed that when the length of the collapsed region in the PCF-SMF-out section was ~110 ± 10 μm, i.e., shorter than the other collapsed region, then the devices exhibited transmission spectra as those shown in Fig. 1. Therefore, we conclude that the dips in the transmission spectra are a result of the overlapping between the excited modes in the PCF. It is important to point out that our devices are different from those based on SMS structures already reported [9–11], [15–24]. Those devices are built also by splicing a segment of fiber into another kind of fiber. In these structures two or several modes are coupled into the spliced fiber at the first junction. At the second junction the modes are recombined. If two modes are excited and recombined the transmission spectrum of the SMS structure exhibits a sinusoidal pattern [9–11], [15–18]. However, if several modes are excited and recombined a single (usually broad) peak or notch is observed [19–24]. The other difference of our devices with other SMF structures already proposed is the overall length and the insertion losses. In our case the length of our devices is around 1 cm while other SMF structures are several centimeters long. The losses in our case are less than 2 dB, contrary to more than 10 dB in some PCF-based interferometers [9–11]. We believe that all those differences and advantages are due to the modal properties of the PCF.

#142479 - $15.00 USD Received 10 Feb 2011; revised 26 Mar 2011; accepted 28 Mar 2011; published 5 Apr 2011

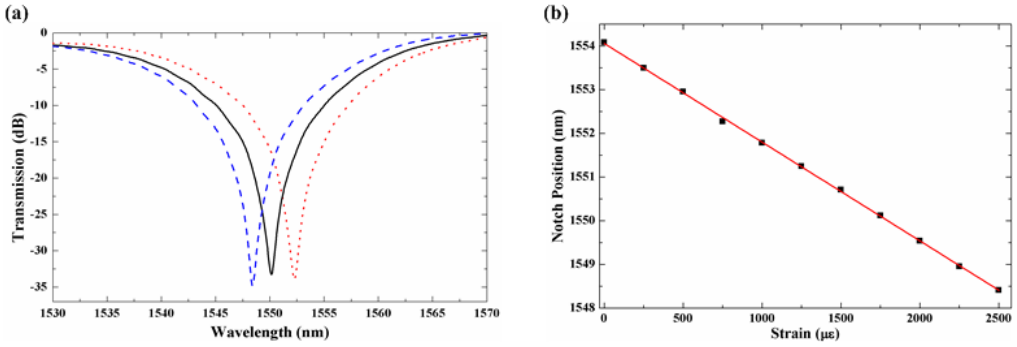

Fig. 3. (a) Transmission spectra at 750 με (dotted line), 1750 με (solid line) and 2500 με (dashed line) observed in a 12 mm-long device. (b). Position of the notch as a function of the applied strain. The measurements were carried out at room temperature.

The sensing properties of individual devices were studied first, particularly to strain and temperature. Basically, these parameters introduce minute changes in the device length or in the modal index which give rise to small changes in the overlapping conditions. As a result, the position of the notches is modified. By correlating the notch position with the parameter being sensed a calibration curve can be obtained. Figure 3 shows the observed transmission spectra of a 12 mm-long device when it was subjected to axial tensile strain. The notch shifts to shorter wavelengths without a significant change in its shape. The figure also shows the position of the notch as a function of the applied strain. A linear behavior can be seen, the correlation factor was found to be $R^2 = 0.9996$. The strain sensitivity was found to be 2.2 pm/με which is about 200% higher than that of a common FBG and comparable to that of other PCF strain sensors based on gratings [3–5] or interferometers [9–14] which in general are more complex or much longer. With available miniature spectrometers or FBG interrogators a shift of 20 pm can be detected. Thus, the estimated strain resolution of the 12 mm-long device is ~10 με. However, in a practical situation the resolution will depend on the interrogation device or on the mechanism to decode the shift of the notch. It is important to point out that several physical parameters such as electric fields, vibration, pressure, load, tilt, etc., can be translated to strain changes. Our devices are sufficient robust to sense these parameters. As point sensor they can provide wavelength-encoded (absolute) and high resolution measurements. Therefore the devices here proposed may be useful in diverse applications of practical interest.

The temperature dependence of the devices was also investigated. It was found that the higher the temperature the longer the notch wavelength. The observed temperature sensitivity was in the 7-9 pm/°C range, depending on the device length. Therefore, the effect on the strain sensitivity of a device at different temperature was investigated. Figure 4 shows the transmission spectra of a 9.52 mm-long device when it was subjected to axial tensile strain

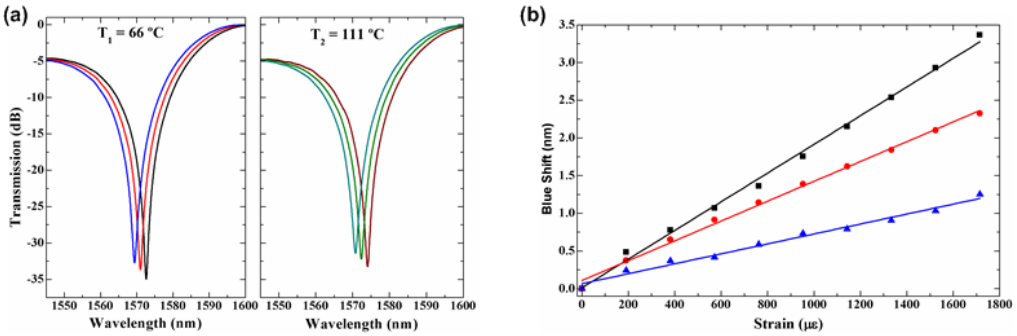

Fig. 4. (a) Transmission spectra of a 9.52 mm-long device subjected to 190, 762, and 1333 με at 66 and 111°C. (b) Shift of the notch as a function of the applied strain at room temperature (squares), 66 °C (dots) and 111 °C (triangles).

#142479 - $15.00 USD Received 10 Feb 2011; revised 26 Mar 2011; accepted 28 Mar 2011; published 5 Apr 2011

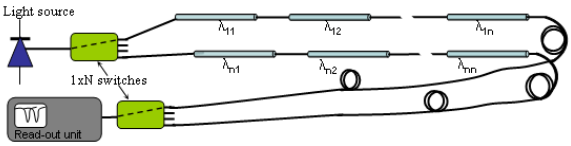

Fig. 5. Schematic representation for multiplexing n sensors. λ_{ni} (i = 1,2,3…n) represent the notch position of the i-th sensor in the n-th fiber.

when the surrounding temperature was 66 or 111°C. The linear behavior is preserved at any temperature within the analyzed range, while the strain sensitivity decreases as the temperature increases. This was expected since strain and temperature induce opposite-sign notch wavelength displacements.

3. Multiplexing capability of the proposed devices

It is recognized by the sensor community that the multiplexing capability of fiber sensors is one of their main advantages. This capability makes it possible to monitor multiple sensing points with a single interrogation unit (composed, e.g., by a single light source and a miniature spectrophotometer), thus significantly reducing the cost and complexity of a sensor array. Most of the SMS-based sensors proposed so far exhibit transmission or reflection spectra with a series of maxima and minima or broad dips/notches which difficult their multiplexing. PCF interferometers, e. g., exhibit sinusoidal interference patterns while PCFs with periodic changes in their structure tend to exhibit broad and irregular dips [8–11]. Thus, when several of these sensors are cascaded one after the other, an overlap of the peaks or dips may occur which imposes complex demodulation schemes or severe constraints in the fabrication of the devices [12–14]. As it can be seen in Fig. 1, our devices exhibit a single and narrow dip in their transmission. Therefore, the multiplexing is quite straightforward - by setting n sensors in a same fiber n dips can be expected. Figure 5 shows a proposed scheme for multiplexing the sensors. In a fiber n sensors can be set in series, all of them can be interrogated simultaneously. To increase the number of sensors in the array two switches can be used. To demonstrate the above concept four sensors were placed in series, the separation between consecutive sensors was around 50 cm. To verify the performance of the sensors when they were in series, each sensor was independently subjected to axial tensile strain. Figure 6(a) shows the composed transmission spectra of the series when one sensor was under strain and the other sensors were not. The shift in only one dip is evident; the other dips remain completely unchanged. Figure 6(b) shows the observed shifts as a function of the applied strain in the four sensors of the series.

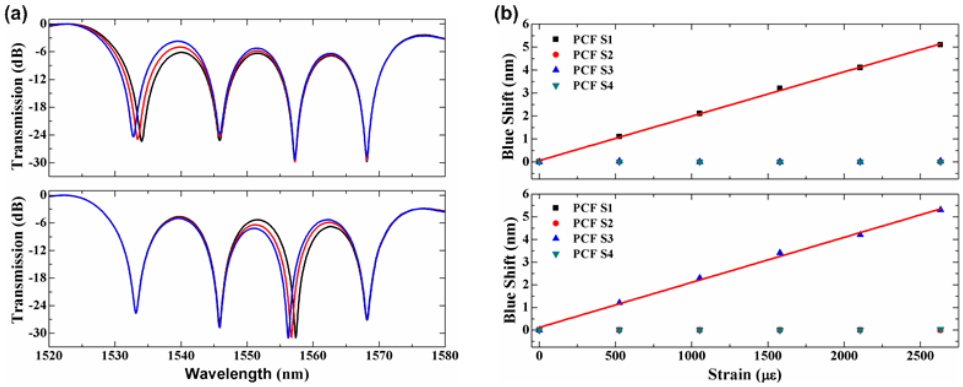

Fig. 6. (a) Normalized transmission spectra observed when four sensors are set in cascade and one of them is subjected to strain. (b) Shift as a function of applied strain observed in the four devices. S1, S2, S3 and S4 refer to sensors 1, 2, 3, and 4, respectively, being 1 the notch at shorter wavelength and 4 the notch at longer wavelength. The lengths of the devices S1, S2, S3, and S4 were, respectively, 10.2, 12.16, 11.9, and 11.42 mm.

#142479 - $15.00 USD Received 10 Feb 2011; revised 26 Mar 2011; accepted 28 Mar 2011; published 5 Apr 2011

Owing to the compactness of the devices the separation between consecutive samples can be as short as a few centimeters (~4-6 cm), provided that the cladding modes of the SMF between the PCFs are stripped out. However, in a practical situation the packaging can impose constraints in the separation between consecutive sensors. The maximum number of sensors that can be set in series will depend, among other factors, on the wavelength span of the light source, the parameter to sense, the measuring range of interest and the overall losses. The measuring range will impose the maximum shift expected while the losses will determined the power budget. For example, if the parameter to measure is strain and the range of interest is ± 1000 με, then a maximum shift of ± 3 nm should be considered in order to avoid overlap between consecutive notches. To estimate a realistic number of sensors that can be set in series, let us assume that the insertion loss of each device is 3 dB, a 10dBm-LED with a span of 100 nm as the light source and that the maximum shift expected is ± 5 nm. Under these conditions, approximately 8 sensors can be cascaded if the read-out or interrogation unit is capable of operating with an input power of around –60 dBm. Therefore with two 1x4 switches an array of more than 30 PCF sensors can be implemented. Such an array can be useful in many practical applications.

4. Conclusions

We have introduced a simple and versatile fiber sensor which consists of a stub of PCF fusion spliced with standard single mode fiber. Two collapsed zones with different lengths in a PCF with adequate structure allow the excitation and overlapping of specific modes in the fiber. The resulting transmission spectrum of the devices exhibits a single, narrow and deep notch, whose position changes with external perturbation, thus making possible the sensing of different parameters. As point sensors the proposed devices are attractive since they provide wavelength-encoded information, are compact, highly sensitive and cost effective. In fact they can be considered a serious alternative to existing PCF sensors as well as to some of those based on conventional fiber. We believe that the results presented here, in particular the multiplexing capability, overcome some of the limitations of PCF based sensors previously reported.

The multiplexing of the proposed sensors is quite straightforward given the fact that, when *n* sensors are placed in series, *n* dips are observed in the transmission. The dips are independent from each other, i.e. a shift of one of them does not affect the position of the others. With commercially available light sources, switches and spectrometers it is feasible to implement an array with tens of sensors. Thus, the exploitation of the PCF sensors here proposed in real applications seems promising.

Acknowledgements

Guillermo Cárdenas is grateful to CONACYT (Mexico) for a PhD Fellowship. This work was supported by the Ministerios de Fomento and de Ciencia e Innovación of Spain under projects SOPROMAC No. P41/08 and TEC2010-14832.

#142479 - $15.00 USD Received 10 Feb 2011; revised 26 Mar 2011; accepted 28 Mar 2011; published 5 Apr 2011